

Acute psychosocial stress alters thalamic network centrality

Janis Reinelt^{a,*}, Marie Uhlig^{a,b,1}, Karsten Müller^a, Mark E. Lauckner^{a,f}, Deniz Kumral^{a,g}, H. Lina Schaare^{a,b}, Blazej M. Baczowski^{a,b,c}, Anahit Babayan^a, Miray Erbey^{a,g,h}, Josefin Roebbig^a, Andrea Reiter^{a,e,i}, Yoon-Ju Bae^d, Juergen Kratzsch^d, Joachim Thiery^d, Talma Hendler^j, Arno Villringer^{a,g}, Michael Gaebler^{a,g}

^a Department of Neurology, Max Planck Institute for Human Cognitive and Brain Sciences, Leipzig, Germany

^b International Max Planck Research School NeuroCom, Leipzig, Germany

^c Institute of Psychology, University of Leipzig, Leipzig, Germany

^d Institute for Laboratory Medicine, Clinical Chemistry and Molecular Diagnostics (ILM) of the Medical Faculty at the University of Leipzig, Leipzig, Germany

^e Lifespan Developmental Neuroscience, Technische Universität Dresden, Dresden, Germany

^f Charité – Universitätsmedizin Berlin, Berlin, Germany

^g MindBrainBody Institute at the Berlin School of Mind and Brain, Humboldt-Universität zu Berlin, Berlin, Germany

^h International Max Planck School on the Life Course, Max Planck Institute for Human Development, Berlin, Germany

ⁱ Max Planck UCL Centre for Computational Psychiatry and Ageing Research, London, United Kingdom

^j School of Psychological Science, Departments of Physiology and Pharmacology and Psychiatry, Faculty of Medicine, Sagol School Neuroscience, Tel Aviv University, Tel Aviv, Israel



ARTICLE INFO

Keywords:

Resting-state fMRI
Eigenvector centrality mapping
Stress
Cortisol
Thalamus
TSST

ABSTRACT

Acute stress triggers a broad psychophysiological response that is adaptive if rapidly activated and terminated. While the brain controls the stress response, it is strongly affected by it. Previous research of stress effects on brain activation and connectivity has mainly focused on pre-defined brain regions or networks, potentially missing changes in the rest of the brain. We here investigated how both stress reactivity and stress recovery are reflected in whole-brain network topology and how changes in functional connectivity relate to other stress measures.

Healthy young males ($n = 67$) completed the Trier Social Stress Test or a control task. From 60 min before until 105 min after stress onset, blocks of resting-state fMRI were acquired. Subjective, autonomic, and endocrine measures of the stress response were assessed throughout the experiment. Whole-brain network topology was quantified using Eigenvector centrality (EC) mapping, which detects central hubs of a network.

Stress influenced subjective affect, autonomic activity, and endocrine measures. EC differences between groups as well as before and after stress exposure were found in the thalamus, due to widespread connectivity changes in the brain. Stress-driven EC increases in the thalamus were significantly correlated with subjective stress ratings and showed non-significant trends for a correlation with heart rate variability and saliva cortisol. Furthermore, increases in thalamic EC and in saliva cortisol persisted until 105 min after stress onset.

We conclude that thalamic areas are central for information processing after stress exposure and may provide an interface for the stress response in the rest of the body and in the mind.

1. Introduction

A typical response to stress involves changes in subjective experience (Hellhammer and Schubert, 2012), in the brain's functional connectivity and activity (van Oort et al., 2017), and in the autonomic nervous as well as the endocrine system (Allen et al., 2017). Through these changes, the acute stress response enables adequate reactions to a stressor. It is

therefore highly adaptive, especially if rapidly activated and rapidly terminated (McEwen and Gianaros, 2011; Steptoe and Kivimäki, 2013). Moreover, an efficient neural processing of stressors is crucial for adapting to future occurrences of similar stressors (Peters et al., 2017). Insufficient initialisation or delayed termination of the stress response ("delayed stress recovery") constitute a major risk factor for mental (Faravelli et al., 2012; Hermans et al., 2014; Pittenger and Duman, 2008)

* Corresponding author. Max Planck Institute for Human Cognitive and Brain Sciences, Stephanstr. 1A, 04103, Leipzig, Germany.

E-mail address: reinelt@cbs.mpg.de (J. Reinelt).

¹ shared first authors.

and physical health (Stephoe and Kivimäki, 2013). Although it is largely acknowledged that brain networks orchestrate the overall stress response and adaptability (Hermans et al., 2014), it remains unclear what circuit guides it (Peters et al., 2017).

Stress-driven changes in the activation and functional connectivity of the brain have been reported in several regions relevant to emotional processing, autonomic control, thoughts, and memory (van Oort et al., 2017). For example, seed-based connectivity analysis of resting-state data acquired after stress exposure showed an increased connectivity of the amygdala – using the averaged time course of bilateral amygdala seeds (Quaedflieg et al., 2015; van Marle et al., 2010) – with multiple regions, including the parahippocampal gyrus and the medial prefrontal cortex (Quaedflieg et al., 2015) as well as the dorsal anterior cingulate (van Marle et al., 2010). Persistent amygdala-hippocampus connectivity, between a bilateral hippocampus seed and amygdala regions, was also related to prolonged subjective stress (Vaisvaser et al., 2013). In another study, elevated connectivity between a bilateral amygdala seed and the posterior cingulate cortex, the ventromedial prefrontal cortex (vmPFC), and the frontal pole until 60 min after stressor offset was found (Veer et al., 2011).

While these studies have shown connectivity changes between predefined subcortical seed regions and the rest of the brain, this region-of-interest (ROI) approach may have missed connectivity between other regions in the brain that are relevant for stress processing. To our knowledge, only two studies so far have investigated neural effects of acute stress at the whole-brain level: Using an independent component approach, which requires a priori definition of the number of components or networks, Hermans et al. (2011) found increased connectivity in regions of the salience network, including anterior insula, inferotemporal cortex, amygdala, and thalamus. Through a pharmacological intervention, blocking either β -adrenergic receptors or cortisol synthesis, the authors could also relate stress-induced connectivity increases to endocrine changes. In another study, Maron-Katz et al. analysed whole-brain functional connectivity using a parcellation-based univariate analysis to show an increased coupling of the thalamus with regions in the frontal, parietal, and temporal lobes after subjects were exposed to a stressful arithmetic task (Maron-Katz et al., 2016). Another study, in which stress was induced through a stressful arithmetic task in the MRI, used the graph-based metrics of “network efficiency” in 106 literature-derived ROIs and of “betweenness centrality” in 12 ROIs (in hippocampus, amygdala, and mPFC) to find a stress-related decrease in “flow of information” (Wheelock et al., 2018).

We here aimed to expand the scope on the stress response in terms of modalities (including psychological, bodily, and brain measures), time (longer sampling period until 105 min after onset of the intervention), and space (voxel-level connectivity analysis), compared to previous stress studies. We chose the Trier Social Stress Test (TSST) as a naturalistic stressor with pronounced, lasting effects on subjective, autonomic, and endocrine stress measures (Allen et al., 2014). To closely control for the study procedure – and particularly for physical activity (standing, walking), which is known to influence endocrine and autonomic parameters (Het et al., 2009) – the so-called “placebo TSST” was chosen as a control intervention (Het et al., 2009). This control procedure involves the same sequence of standing, sitting, talking, and calculating as the TSST but without the social stress of a committee. To investigate stress-related changes in functional network topology, Eigenvector centrality (EC) mapping (ECM) was applied (Lohmann et al., 2010). ECM is an exploratory and data-driven whole-brain approach that allows the quantification of the importance of network nodes with a voxel-wise resolution and without the need to preselect specific ROIs. In contrast to other centrality measures (e.g., [within-module] degree centrality), EC uses all correlations of the adjacency matrix, that is, it not only regards direct connections but integrates information about all linked regions. To maximally capture the large-scale effects of stress on brain functional connectivity (Hermans et al., 2014), the whole-brain approach of ECM was chosen. Voxels and regions with high EC can be considered

“influential hubs” within a network, which facilitate functional integration and are essential to network resilience under stress perturbation (Joyce et al., 2010; Rubinov and Sporns, 2010).

In this study, we aimed to (1) investigate stress reactivity in the brain and hypothesized immediate stress-driven effects on whole-brain network topology, based on previous findings of functional connectivity changes after stress (Hermans et al., 2014; van Oort et al., 2017). We also aimed to (2) explore the association between neural stress reactivity and other dimensions of the stress response, expecting a correlation with subjective stress ratings as well as with autonomic (heart rate and its variability) and – particularly – endocrine stress markers (i.e., cortisol) (Hermans et al., 2014). Finally, we aimed to (3) characterize the time course of stress-induced brain connectivity alterations by extending the sampling window to the point at which stress-related changes in functional connectivity are assumed to recover (i.e., 60–90 min after stress onset or approximately 40–70 min after stress offset; Hermans et al., 2014).

2. Methods

2.1. Participants

Male participants between 18 and 35 were recruited via leaflets, online advertisements, and from a database at the Max Planck Institute for Human Cognitive and Brain Sciences in Leipzig, Germany. We limited the sample to male participants, since the female reproductive cycle impacts stress hormone levels (Childs et al., 2010). Prior to the stress study, participants were tested according to the protocol of the MPI-Leipzig Mind-Brain-Body database that comprised cognitive testing, blood screening, anthropometric measurements, structural and resting-state functional MRI scans, resting-state electroencephalography (EEG), self-report questionnaires, and a structured clinical interview (for details, cf. Babayan et al., 2019; Mendes et al., 2019). A pre-screening was conducted via telephone with the following exclusion criteria: smoking, excessive alcohol or drug consumption, past or present enrolment in a psychology study programme, no previous exposure to the TSST or similar stress experiments, regular medication intake, history of cardiovascular, psychiatric, or neurological diseases, or body mass index higher than 27 kg/m². For magnetic resonance imaging (MRI), standard MRI exclusion criteria additionally applied (e.g., tattoos, irremovable metal objects such as retainers or piercings, tinnitus, or claustrophobia). For details, cf. Babayan et al. (2019) and Mendes et al. (2019). 67 participants were included in the study and randomly assigned to either the TSST (n = 33) or the control group (n = 34). Written informed consent was obtained from all participants. The study was approved by the ethics committee at the Medical Faculty of the University of Leipzig (number 385-1417112014). Participants received a financial compensation for their participation.

2.2. Procedure

For an overview of the whole procedure, see Fig. 1. Appointments were scheduled at the same time of day (11:45 am) to control for diurnal fluctuations of hormones (e.g., cortisol). Participants were asked to get at least 8 h of sleep before the day of the experiment, to get up no later than 9 am, to have a normal breakfast, and then refrain from eating until their appointment. Additionally, participants were asked not to exercise or to consume stimulant drinks like coffee or black tea before their study appointment, since caffeine intake may alter the hypothalamic-pituitary-adrenal axis response (al'Absi et al., 1998) and resting-state measures (Rack-Gomer et al., 2009). The experimental staff was blind to the participant's group assignment before the intervention, after which they did not communicate with the participant (until the second anatomical scan). Throughout the experiment, there were fifteen time points (T0-T14) at which saliva samples and subjective measures were collected and 14 time points (T1-T14) at which blood samples were collected. After a short

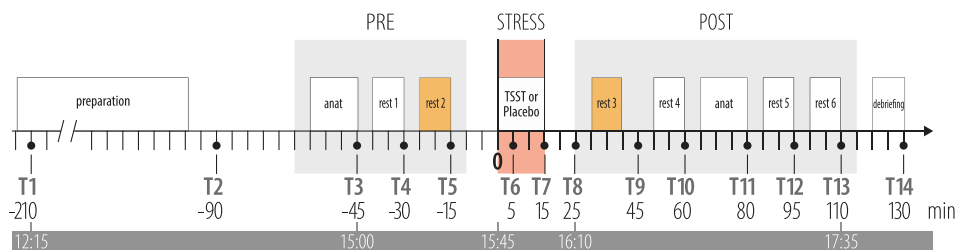


Fig. 1. Experimental design. Between-subject design with one group ($n = 33$) undergoing the Trier Social Stress Test (TSST) and the other ($n = 34$) a “placebo” TSST. Six 8-min blocks of resting-state fMRI were acquired: two before (*rest1*, *rest2*) and four after the intervention (*rest3*–*rest6*). During resting-state fMRI, participants were instructed to fixate a crosshair. Psychometric ratings, saliva, and blood samples were acquired at 14 time points throughout the experiment (T1–T14). The hours indicate the time at which important sampling points were scheduled. Heart rate was recorded inside and outside the scanner. The resting-state blocks before (*rest2*) and after (*rest3*) the intervention (labelled in orange) were used for the analysis of stress reactivity. White boxes labelled “anat” represent sequences of cerebral blood flow (pulsed arterial spin labelling; results reported elsewhere) and high-resolution anatomical image acquisition (MP2RAGE). The grey boxes indicate phases in the MRI. The TSST and the control condition took place outside of the scanner.

period of familiarisation to the experimental environment, signing consent forms, and receiving instructions, participants chewed on a first Salivette swab (Sarstedt AG & Co. KG, Nümbrecht, Germany) while they answered questions about their current subjective experiences (T0). The second psychometric and saliva sample were acquired together with the first blood sample, after participants were equipped with an intravenous catheter and the portable electrocardiography (ECG) device (T1, 210 min before TSST onset). Participants then gave a urine sample before they had a 15-min break, during which they received a standardised lunch. Participants then filled out self-report trait questionnaires (see below and Table S2) and rested for 30 min, before sampling instance T2 followed (90 min before TSST onset). Afterwards, participants completed the pre-intervention scanning session, consisting of a quin pilot (to plan details like the slice positioning of the subsequent image acquisition), a pulsed arterial spin labelling (pASL) scan (the results of which will be reported elsewhere), a high-resolution anatomical scan (MP2RAGE), and two resting-state (RS) scans (T2*-weighted EPI). While participants were in the MRI, they completed two more sampling instances: T3 between the MP2RAGE and the first RS scan (45 min before TSST onset) as well as T4 between the two successive RS scans (30 min before TSST onset). After the baseline RS scan (*rest2*, 25 min before TSST onset), sampling instance T5 followed in the MRI (15 min before TSST onset). Participants were then brought to the testing room, where they underwent either the TSST or the “placebo” TSST (cf. Next section and supplementary material for details). During the intervention, there were two sampling instances: T6 (+5 min after TSST onset) and T7 (+15 min after TSST onset). Following the intervention, participants were brought back to the MRI, where sampling instance T8 (+25 min after TSST onset) followed. The post-intervention scan protocol consisted of a second quin pilot, two RS scans (*rest3*, +30 min after TSST onset, and *rest4*, +50 min after TSST onset), a second pASL scan, a second high-resolution anatomical scan (MP2RAGE), again followed by two RS scans (*rest5*, +85 min after TSST onset, and *rest6*, +105 min after TSST onset). Between the sequences, there were sampling instances T9 (+45 min after TSST onset), T10 (+60 min after TSST onset), T11 (+80 min after TSST onset), T12 (+95 min after TSST onset), and T13 (+110 min after TSST onset). For the sampling instances between the scans, participants stayed within the MRI bore and the scanner bed was not moved. The Salivette was placed inside the participant’s mouth through the bore opening close to his head. Blood drawing inside the scanner was accomplished through a tube attached to the intravenous catheter. Following the last RS scan, participants left the

MRI and completed a post-event processing questionnaire (Fehm et al., 2008), the results of which will be presented elsewhere. In the end, participants were brought to a separate room, where they were debriefed. The experiment ended with final sampling instance T14 (+130 min after TSST onset).

2.3. Stress and control intervention

To elicit a pronounced stress response, which is required for the study of its time course (Linden et al., 1997), we chose the Trier Social Stress Test (TSST) as one of the strongest and most naturalistic stressors applicable in humans (Kirschbaum et al., 1993). To tightly control for physical and cognitive load, the “placebo” TSST was selected as the control task (Het et al., 2009; Kirschbaum et al., 1993). A detailed description of both conditions can be found in the supplementary material. After participants in the TSST group had finished the mental arithmetics, they were told that another task would follow in the MRI; to maximize and extend the psychological and physiological effects of the TSST. They were then brought back to the scanning area in the company of the experimenter and the committee members. After *rest4* (+60 min after TSST onset), they were told that no additional task would follow and that they could relax.

2.4. Psychometric data

Throughout the experiment, subjective ratings were collected at 15 time points (T0–T14, see Fig. 1). Except for the first two (T0, T1), all sampling instances followed the same procedure: questionnaires were presented with OpenSesame 3.1.2 (Mathôt et al., 2011) on a laptop screen (outside the scanner) or on the MRI screen (inside the scanner). Participants answered the questionnaires with the laptop keyboard (outside the scanner) or an MRI-compatible button box (inside the scanner). Subjective experience was measured using an affect grid (Killgore, 1998), the state trait anxiety questionnaire (STAI, state subscale, Grimm et al., 2009; Spielberger, 1983), the “current mood scale” (“Aktuelle Stimmungsskala” (Dalbert, 1992), and a set of individual questions (e.g., “How stressed do you feel right now?”), which were answered using visual analogue scales (VAS) with sliding bars from 0 (“not at all”) to 100 (“very much”). For details cf. Table S1.

In addition to the psychometric assessment of subjective state measures, participants completed self-report trait questionnaires during the

relaxation period prior to the first MRI measurement (between T1 and T2). These included the Trier Inventory of Chronic Stress (Schulz and Schlotz, 1999), the Perceived Stress Scale (Klein et al., 2016), and questions regarding individual sportive activity and sleep quality (for details cf. Table S2).

For the analysis of subjective experience, we focused on the measures most relevant to subjective stress and used in previous stress studies (e.g. Allen et al., 2014; Hellhammer and Schubert, 2012): That is, anxiety and subjective stress at each sampling time point were quantified using the STAI sum score and the VAS value of the question “How stressed do you feel right now?”, respectively. Results of other psychometric measures will be reported elsewhere.

2.5. Autonomic data

To measure heart rate (HR) and its variability (HRV), electrocardiography (ECG) and photoplethysmography (PPG) were recorded. Outside the MRI, a 1-channel ECG was recorded (at 250 Hz) using a BioHarness3 (Zephyr, Annapolis, Maryland, US) strap attached to the participants' chests at the height of the xiphoid process. Inside the MRI, ECG was recorded (at 1000 Hz) using an MR-compatible BrainAmp ExG MR amplifier (Brain Products GmbH, Gilching, Germany) with Power-Pack battery, SyncBox synchronization interface and the acquisition software BrainVision Recorder (Version 1.20). To reduce artifacts related to breathing (i.e., movement of the thorax), three electrodes were placed on the participants' backs (adjacent to cervical spine c7, above the coccyx, and 15 cm below the left armpit). Also in the MRI, PPG was recorded (at 1000 Hz) using an OXY100C pulse oximeter module with TSD123A finger clip transducer and a BIOPAC MP150 system with the acquisition software AcqKnowledge (Version 4.0, BIOPAC Systems Inc., Goleta, CA, USA).

For the analysis of HR and HRV, the time series were binned into intervals of 3 min. This resulted in two intervals per RS scan and one interval for each phase of the TSST (“anticipation”, “interview”, “arithmetic”). For ECG data acquired during RS fMRI, gradient artefacts were removed using a self-built template-based subtraction method in Matlab (Nierhaus et al., 2013). For ECG and PPG data, peaks were automatically detected and – if needed – manually corrected (less than 1% of peaks) upon visual inspection using Matlab's *findpeaks* function or Kubios 2.2 (Tarvainen et al., 2014). For each interval, either PPG or ECG data were used for HR/V analysis: For data acquired in the MRI, the PPG data was used unless when missing (in total 37 intervals) or when the number of faulty, manually uncorrectable peaks (due to wrong detection and/or artefacts) exceeded 5% (in total 40 intervals); then, the ECG data for that interval were analysed instead. The heart period (average interbeat interval length in ms or inverse HR) was determined for each interval and HRV was quantified as root mean square of successive differences (RMSSD), indexing parasympathetic cardio-regulation (e.g. Berntson et al., 1997).

2.6. Endocrine data

In parallel to the subjective ratings, blood and saliva samples were obtained at 14 time points throughout the procedure (T1–T14, also see Fig. 1). While participants were responding to the questionnaires, saliva was sampled with a Sarstedt Salivette (duration: at least 2 min). During the subjective sampling, the experimenter acquired blood samples (serum and plasma, Sarstedt Monovette) from the intravenous catheter in the left or right cubital vein. Samples were centrifuged and aliquoted for the quantitative analysis. Cortisol concentrations in saliva were determined using Liquid chromatography-tandem mass spectrometry (LC-MS/MS) at the Institute for Laboratory Medicine, Clinical Chemistry and Molecular Diagnostics, University of Leipzig, following the protocol described in (Gaudl et al., 2016). For a different focus of the study, other endocrine markers in blood and serum were measured (results reported in Bae et al., 2019).

2.7. Neuroimaging data

Magnetic resonance imaging (MRI) was performed on a 3 T S MAGNETOM Verio (Siemens, Erlangen, Germany) scanner using a 32-channel Siemens head-coil. High resolution structural MR images were acquired using an MP2RAGE sequence: sagittal acquisition orientation, one 3D volume with 176 slices, repetition time (TR) = 5000 ms, TE = 2.92 ms, TI1 = 700 ms, TI2 = 2500 ms, FA1 = 4°, FA2 = 5°, pre-scan normalization, echo spacing = 6.9 ms, bandwidth = 240 Hz/pixel, FOV = 256 mm, voxel size = 1 mm isotropic, GRAPPA acceleration factor 3, slice order = interleaved, duration = 8 min 22 s (Marques et al., 2010). Six blocks (see Fig. 1) of 8-min RS fMRI (336 vol) were acquired using a T2*-weighted echo planar imaging (EPI) sequence: axial acquisition orientation, phase encoding = A >> P, voxel size = 2.3 mm isotropic, FOV = 202 mm, imaging matrix = 88 x 88, 64 slices with 2.3 mm thickness, TR = 1400 ms, TE = 30 ms, flip angle = 69°, echo spacing = 0.67 ms, bandwidth = 1776 Hz/pixel, partial fourier 7/8, no pre-scan normalization, multiband acceleration factor = 4, 336 vol, slice order = interleaved, duration = 7 min 50 s. During each RS scan, participants were instructed to lie still with their eyes open and to loosely fixate a low-contrast crosshair. Before each RS scan, a pair of gradient echo non-EPI scans (TR = 0.68 s, TE1 = 5.19 ms, TE2 = 7.65 ms, flip angle = 60°, voxel size = 2.3 mm isotropic, FOV = 202 mm, 64 slices) and two sets of spin echo EPI scans (TR = 2.2 s, TE = 50 ms, flip angle = 90°, multiband factor = 4, voxel size = 2.3 mm isotropic, FOV = 202 mm, 64 slices, phase encoding = AP, 3 vol/PA, 3 vol) were acquired for field map and reverse phase encoding distortion correction, respectively. FMRIB Software Library FSL (Smith et al., 2004) was used for all preprocessing steps except for spatial transformations, which were performed with Advanced Normalization Tools (ANTs; Avants et al., 2011). To ensure a standardised and reproducible procedure, the complete pipeline (https://github.com/NeuroanatomyAndConnectivity/pipelines/tree/master/src/lzd_lemmon) was implemented in Nipype (Gorgolewski et al., 2011). Preprocessing of the RS data fMRI comprised: discarding the first 5 vol, realignment, distortion correction, denoising (motion parameters and physiological noise), co-registration to the T1-weighted high resolution image, high pass filtering (0.01 Hz), spatial smoothing with a 6 mm full-width-at-half-maximum (FWHM) kernel, and normalisation to standard space (MNI152). A detailed description of the preprocessing pipeline can be found in the supplementary material.

Quality reports for all RS scans were created using a customized Nipype workflow described in Mendes et al. (2019) and are available at https://github.com/NeuroanatomyAndConnectivity/pipelines/tree/master/src/lzd_lemmon. Quality assessment (QA) included the calculation of motion parameters such as framewise displacement (calculated as the sum of the absolute values of the six realignment parameters), and the visual assessment of co-registration quality, and temporal signal-to-noise (tSNR). Each individual's scan quality scores were compared to the group-level distribution and for each scan, the QA report was visually inspected to ensure adequate data quality (cf. “Data availability”).

2.7.1. Eigenvector centrality mapping

To assess stress-related changes in the topology of whole-brain functional connectivity, Eigenvector centrality (EC) mapping (ECM; Lohmann et al., 2010) was used. The graph-analytic metric EC quantifies the importance of individual nodes (here: voxels) within a network (Joyce et al., 2010; Rubinov and Sporns, 2010), that is, high EC indicates that a node is highly connected to other nodes of the network, which are themselves highly connected. ECM allows an exploratory whole-brain approach independent from predefined seed regions (Lohmann et al., 2010). Voxelwise ECMs were calculated (for each RS scan) using the fast ECM algorithm (Wink, de Munck, van der Werf, van den Heuvel and Barkhof, 2012).

2.8. Statistical analysis

2.8.1. Data availability

From the analysis of the MRI data, six participants were excluded: four due to excessive head movement (criterion: at least one volume with >2.3 mm [voxel length] of framewise displacement; Power et al., 2012) in the RS scans immediately before (*rest2*) or after (*rest3*) the intervention, one participant aborted the scan, and one participant was excluded because of an incidental finding that was discovered after the data acquisition was completed. Imaging data from 29 participants in the stress and 32 participants in the control group were analysed. From the analysis of EC, psychometric, autonomic, and endocrine data using linear mixed models, an additional participant in the stress group was excluded because of a cortisol increase below 1.5 nmol/l, which is considered a non-responder (Miller et al., 2013). For the correlations between brain measures and subjective or autonomic stress markers within the stress group, participants with missing data points at either *rest2* or *rest3* were excluded: None for psychometric data (total $n = 28$) and three for HR/VP analysis due to mis-sampled ECG/PPG data (total $n = 26$).

For the endocrine data, two single missing sampling time points (T8, in the stress group) were imputed with the mean of the values before and after the missing value. In total, cortisol data from 28 participants were analysed.

2.8.2. Group-level analysis of EC maps

Differential effects of the intervention on both groups were analysed using a “flexible factorial” model in SPM12 (Wellcome Trust Centre). ECMs from *rest2* (immediately before the intervention) and *rest3* (immediately after the intervention, i.e., +30 min after its onset) were entered into a model including the factors *pre-post* (*rest2*, *rest3*; within-subject), *group* (stress, control; between-subject), and *subject*. We defined contrasts which tested the interaction of *time point* and *group*, as well as the simple effect of *time point*, within the stress and the control group, respectively. To specify stress-related EC changes, the ECMs of the time point by group interaction and of the simple effect of time point in the stress group were overlaid using FSLmaths. The resulting mask was binarized and used to extract EC values from all participants and scans (*rest1* to *rest6*), which were then correlated with psychometric, endocrine, and autonomic data.

All maps were corrected for multiple comparisons using a cluster-level family wise error (FWE) correction (Nichols and Hayasaka, 2003) with a threshold of $p < 0.005$ (uncorrected) at the voxel-level and of $p < 0.05$ (FWE-corrected) at the cluster-level (Bansal and Peterson, 2018; Mueller et al., 2017). The cluster extent (k_E) threshold was set using the tool SPM_ClusterSizeThreshold (Phillips, 2016), yielding a cluster extent threshold of $k_E = 251$. To investigate the network of stress-related EC changes, an exploratory seed-based functional connectivity was performed (cf. Supplement for methods and results).

2.8.3. Linear mixed models of stress measures

To investigate the time courses of EC values and other (i.e., psychometric, autonomic, and endocrine) measures across all RS scans (*rest1* to *rest6*), linear mixed models (Baayen, R Harald, 2008; Brown et al., 2014) were computed using the function *lmer* of the package *lme4* (version 1.1–13; Bates et al., 2015) in R 3.0.2 (R Core Team, 2008). To test whether the measures of interest were specifically influenced by stress (i.e., the interaction of *RS-scan* and *group*), the model included the respective measure as the outcome variable and *RS-scan* as well as *group* as fixed effects. To correct for differences in baseline values, these were included (average values during *rest2*) as a fixed effect. To control for the repeated measures, “participant” was included as a random intercept. Significance of the full model was determined by comparing it to a reduced model without the interaction of *RS-scan* and *group* using a likelihood ratio test (R function *anova* with argument *test* set to “Chisq”; Dobson and Barnett, 2018; Forstmeier and Schielzeth, 2011). In case of a significant difference between the full and the reduced model, post-hoc

least-squares means tests, adjusted for multiple comparisons using Tukey’s method, were performed with the R-package *emmeans* (version 1.1.2.; Lenth et al., 2018). Prior to analyses, the data were inspected, the required assumptions were tested, and parametric variables were z -transformed (see supplementary material for details).

2.8.4. Correlations between brain measures and other stress markers

To analyse the relationship between stress-related changes in EC values and the other (psychometric, autonomic, and endocrine) stress markers, their deltas were computed by subtracting *rest2* values from *rest3* values and correlated using Spearman’s rank correlation (due to the non-normality of EC values; Shapiro-Wilk test: $W(29) = 0.87$, $p = 0.002$) in R 3.0.2 (R Core Team, 2008). As psychometric (state anxiety, subjective stress) and endocrine (salivary cortisol) stress markers were not acquired during the fMRI sequence but before and after each RS scan, the two values were averaged before the delta between *rest2* and *rest3* was created. For the heart rate data, the two 3-min intervals during the RS scans were averaged before the correlation.

3. Results

The stress and the control group did not differ significantly in age, hours of sleep before the day of the experiment, average sportive activity per week, or self-reported chronic stress (see Table S5).

3.1. Psychometric, autonomic, and endocrine results

In response to the TSST, the stress group showed significantly different reactions in psychometric (state anxiety and subjective stress), autonomic (HR and HRV), and endocrine (salivary cortisol) stress markers compared to the control group (Fig. 2).

3.1.1. State anxiety and subjective stress

For state anxiety (STAI) scores, there was a significant interaction between *RS-scan* and *group* ($\chi^2(5) = 27.62$, $p < 0.001$). Post-hoc tests showed significant group differences at *rest3* (+35 min, t-ratio (272.59) = -3.13 ; $p < 0.01$; stress > control group), and *rest6* (+105 min, t-ratio (272.59) = 2.20; $p < 0.05$; control > stress group). For subjective stress (VAS “stressed”), there was a significant interaction between *RS-scan* and *group* ($\chi^2(5) = 15.19$, $p < 0.01$). Post-hoc tests did not show significant group differences at *rest3* (+35 min, t-ratio (303.44) = -1.57 ; $p = 0.11$) but at *rest6* (+105 min, t-ratio (303.44) = 2.60; $p < 0.01$; control > stress group).

3.1.2. Heart rate and heart rate variability

For HR changes, there was a significant interaction between *RS-scan* and *group* ($\chi^2(5) = 74.94$, $p < 0.001$). Post-hoc tests revealed significant group differences (stress > control group) in HR at *rest3* (+35 min, t-ratio (180.67) = -7.96 ; $p < 0.0001$), *rest4* (+55 min, t-ratio (180.67) = -5.4 ; $p < 0.0001$), *rest5* (+90 min, t-ratio (180.67) = -3.87 ; $p < 0.001$), and *rest6* (+105 min, t-ratio (184.36) = -4.48 ; $p < 0.0001$). For HRV measured as RMSSD changes, there was a significant interaction between *RS-scan* and *group* ($\chi^2(5) = 15.68$, $p < 0.01$). Post-hoc tests revealed significant group differences (control > stress group) in RMSSD at *rest3* (+35 min, t-ratio (220.13) = 2.95; $p < 0.01$) and *rest6* (+105 min, t-ratio (223.84) = 2.24; $p < 0.05$).

3.1.3. Saliva cortisol

For saliva cortisol there was a significant *RS-scan* by *group* interaction ($\chi^2(5) = 183.62$, $p < 0.001$) driven by significant group difference (stress > control group) for all RS scans after stress exposure, at *rest3* (+35 min, t-ratio (232.35) = -12.64 ; $p < 0.0001$), *rest4* (+55 min, t-ratio (232.35) = -11.75 ; $p < 0.0001$), *rest5* (+90 min, t-ratio (232.35) = -7.75 ; $p < 0.0001$), and *rest6* (+105 min, t-ratio (232.35) = -6.48 , $p < 0.0001$).

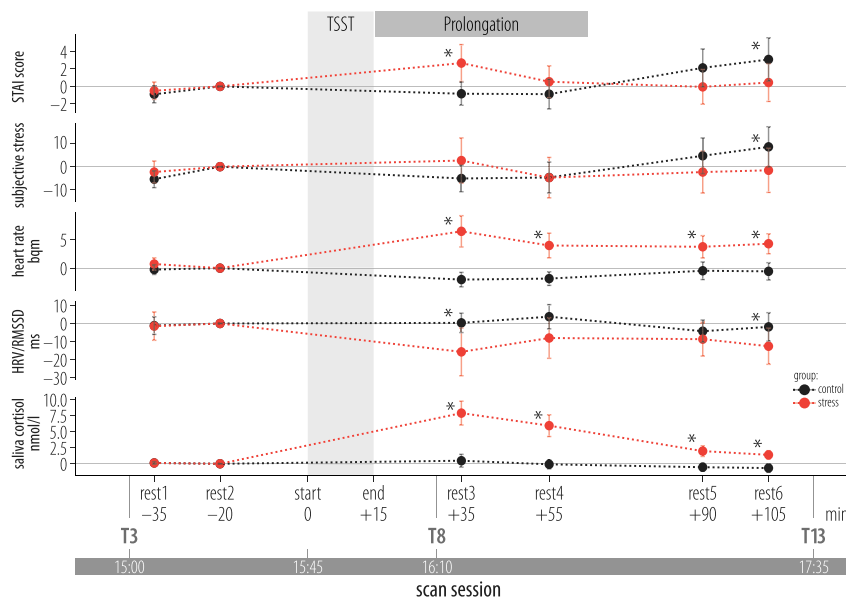


Fig. 2. Mean time courses of state anxiety (STAI), subjective stress (VAS, “stressed”), heart rate (HR, in beats per minute, bpm), heart rate variability (HRV, as root mean square of successive differences, RMSSD, in ms), and saliva cortisol (in nmol/l), plotted over the six resting-state (RS) scans (baseline-corrected with the values of *rest2*). Timing relative to TSST (start, end, darker grey area). The lighter grey area highlights the time when participants in the stress group were still expecting another task (see section 2.3). After *rest4* (+60 min after TSST onset), they were told that no additional task would follow and that they could relax. The hours indicate the time at which important sampling points were scheduled. Linear mixed models show significant *RS-scan* by *group* interactions for all five measures. For visualization purposes and to be comparable to the brain measure of Eigenvector centrality, the values were down-sampled by taking the mean per RS scan. See Fig. S1 for the time courses over all 14 time points. Error bars: 95% confidence interval. * = $p < .05$.

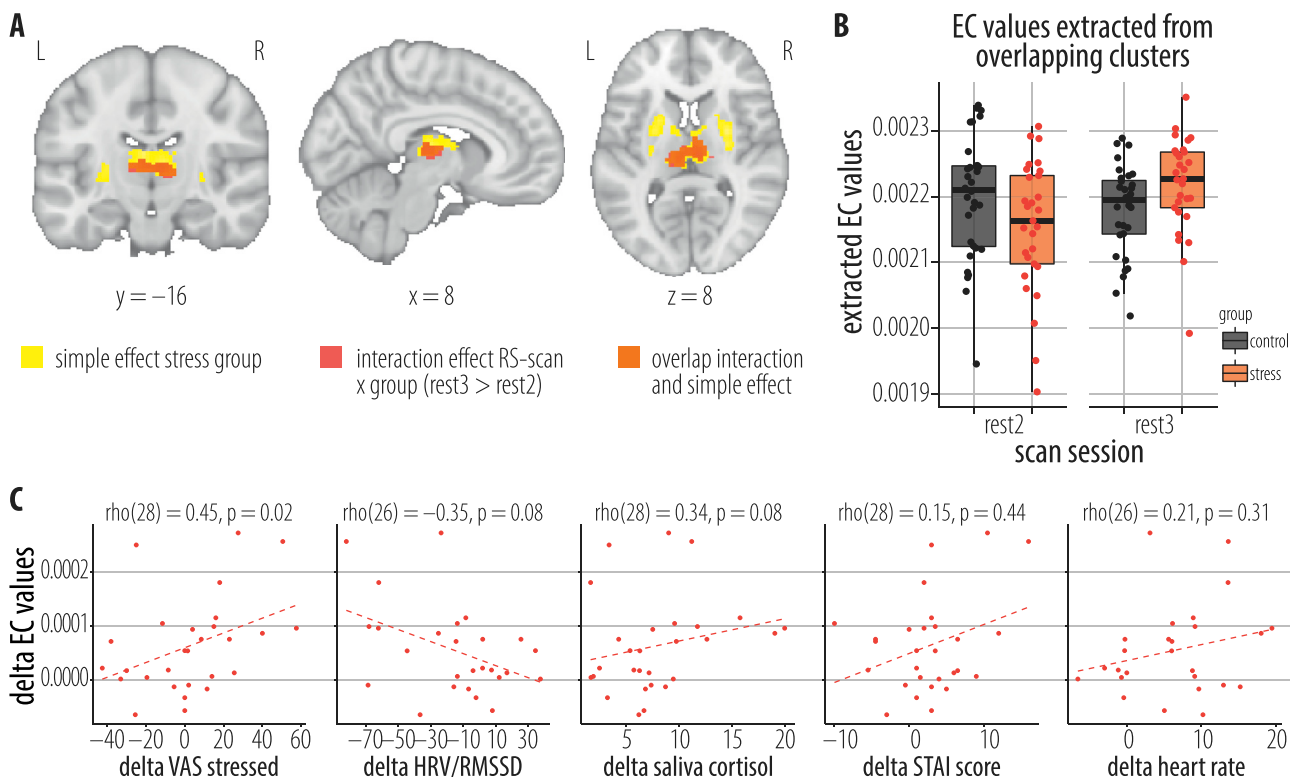


Fig. 3. Changes in Eigenvector centrality (EC) after an acute stressor and their association with other stress markers. **(A)** Significant clusters of increased EC, *rest2* (20 min before the stressor) < *rest3* (+35 min after the stressor). The overlap between the *RS-scan* by *group* interaction and the simple effect of *RS-scan* in the stress group (which almost completely overlaps the cluster of the simple effect) was located in the bilateral thalamus. Threshold: $p < 0.005$ (uncorrected) at the voxel and $p < 0.05$ (FWE-corrected) at the cluster level. **(B)** Box plots (horizontal bar: median; whiskers: 1.5 interquartile range; dots: data from individual participants) of the extracted EC values from the overlap of simple and interaction effect depicted in (A) plotted for *rest2* and *rest3* in the stress (red) and control (black) group. **(C)** Stress-related EC increases in the subcortical cluster (overlap simple and interaction effect) significantly correlated (Spearman’s rank correlation on deltas between *rest3* and *rest2*) with other stress measures in the stress group: (top left) positively with subjective stress (visual analogue scale, VAS, “How stressed do you feel right now?”), (top middle) negatively with heart rate variability (HRV, measured as root mean squared successive differences, RMSSD, in ms), and (top right) positively with saliva cortisol (in nmol/l) but not with (bottom left) state anxiety (STAI) or (bottom right) heart rate. Dashed lines support visual estimation.

3.2. Neuroimaging results

The interaction of *pre-post* (*rest2*, *rest3*) and *group* (stress, control) was

significant in subcortical and frontal clusters. In the stress group (compared to the control group), EC in a subcortical cluster around the bilateral thalamus (peak MNI coordinate: [−6, −26, 2], $T = 4.14$,

$p_{FWE} = 0.011$, $k_E = 335$; see Fig. 3A, see Table 1), increased from pre-stress (*rest2*, 20 min before TSST onset) to post-stress (*rest3*, +35 min after TSST onset). Significant clusters of increased EC in the simple effect in the stress group overlapped with the clusters of the interaction effect and showed a wider extension to bilateral putamen and caudate nucleus (MNI coordinate: $[-26, 12, -6]$, $T = 5.24$, $p_{FWE} < 0.001$, $k_E = 545$; and MNI coordinate: $[28, 14, -8]$, $T = 4.5$, $p_{FWE} < 0.001$, $k_E = 1336$, respectively, see Table 1). The simple effect in the stress group also showed a significant cluster of increased EC in the bilateral cerebellum

Table 1
Stress-related increases in subcortical Eigenvector centrality.

| Contrast | cluster/ extent (n voxels) | Region | Peak Voxel coordinates (MNI) | | | T max |
|---|----------------------------------|------------|--|-------------------|----------|----------|
| | | | x | y | z | |
| | | | Interaction stress vs. control (<i>pre-post</i> by group) | Cluster 1/ 335 | Thalamus | |
| | | Maximum 1 | -6 | -26 | 2 | 4.14 |
| | | Maximum 2 | 8 | -14 | 6 | 3.86 |
| | | Maximum 3 | -4 | -16 | 8 | 3.69 |
| | | Maximum 4 | 18 | -20 | 6 | 3.44 |
| | | Maximum 5 | 4 | -4 | 4 | 2.94 |
| Simple effect in stress group (<i>rest2 < rest3</i>) | Cluster 1/ 1336 | Thalamus | | | | |
| | | Maximum 1 | 28 | 14 | -8 | 4.50 |
| | | Maximum 2 | 28 | 6 | -2 | 4.32 |
| | | Maximum 3 | -8 | -18 | 8 | 4.29 |
| | | Maximum 4 | 28 | 0 | 8 | 4.19 |
| | | Maximum 5 | 10 | 0 | 18 | 4.16 |
| | | Maximum 6 | -4 | -16 | 16 | 4.08 |
| | | Maximum 7 | -6 | -20 | 10 | 3.89 |
| | | Maximum 8 | 28 | -10 | 10 | 3.87 |
| | | Maximum 9 | 16 | 0 | 18 | 3.70 |
| | | Maximum 10 | 12 | -4 | 14 | 3.68 |
| | | Maximum 11 | 26 | 4 | -10 | 3.67 |
| | Cluster 2/ 766 | Cerebellum | | | | |
| | | Maximum 1 | -16 | -72 | -24 | 4.28 |
| | | Maximum 2 | -36 | -62 | -28 | 4.26 |
| | | Maximum 3 | -44 | -70 | -14 | 4.03 |
| | | Maximum 4 | -6 | -70 | -34 | 3.90 |
| | | Maximum 5 | -16 | -48 | -24 | 3.82 |
| | | Maximum 6 | -38 | -58 | -40 | 3.76 |
| | | Maximum 7 | -24 | -60 | -30 | 3.66 |
| | | Maximum 8 | -32 | -70 | -24 | 3.37 |
| | | Maximum 9 | -10 | -56 | -28 | 3.34 |
| | | Maximum 10 | -32 | -76 | -30 | 3.32 |
| | | Maximum 11 | -18 | -66 | -32 | 3.26 |
| | Cluster 3/ 545 | Putamen | | | | |
| | | Maximum 1 | -26 | 12 | -6 | 5.24 |
| | | Maximum 2 | -26 | 2 | -2 | 4.44 |
| | | Maximum 3 | -22 | 6 | 6 | 3.92 |
| | | Maximum 4 | -26 | 0 | 6 | 3.89 |
| | | Maximum 5 | -18 | 8 | 20 | 3.60 |
| | | Maximum 6 | -26 | -16 | 6 | 3.50 |
| | | Maximum 7 | -12 | 14 | 14 | 3.22 |
| | | Maximum 8 | -32 | -8 | -4 | 3.19 |
| | | Maximum 9 | -28 | -10 | 14 | 2.95 |
| | | Maximum 10 | -30 | -10 | -14 | 2.77 |
| | | Maximum 11 | -8 | 10 | 12 | 2.74 |

(MNI coordinate: $[-16, -72, -24]$, $T = 4.28$, $p_{FWE} < 0.001$, $k_E = 766$, see Table 1). Furthermore, the interaction contrast for testing the decrease of EC within the stress group revealed a significant cluster in the frontal pole (MNI coordinate: $[8, 62, -4]$, $T = 4.18$, $p_{FWE} = 0.005$, $k_E = 374$, see Table 1). However, this did not overlap with any simple effect. The simple effect in the control group showed a significant EC increase in a cluster around the left lateral temporal pole (MNI coordinate: $[30, -30, -32]$, $T = 5.27$, $p_{FWE} < 0.05$, $k_E = 276$, see Table 1) and a decrease in occipital cluster (MNI coordinate: $[4, -88, 8]$, $T = 5.22$, $p_{FWE} < 0.001$, $k_E = 1427$, see Table 1). Both clusters did not overlap with significant clusters in the interaction analysis.

The exploratory seed-based analysis yielded widespread connectivity increases between the thalamic cluster and parietal as well as temporal regions in the stress group (cf. Fig. S3), including bilateral hippocampus and amygdala.

3.3. Associations between stress measures

For delta values (*rest3-rest2*) in the stress group, EC showed a significant positive correlation with both subjective stress ($\rho(28) = 0.45$, $p = 0.02$). The positive correlation between saliva cortisol and EC showed a non-significant trend ($\rho(28) = 0.34$, $p = 0.08$). Similarly, the negative correlation between HRV/RMSSD and EC showed a non-significant trend ($\rho(26) = -0.35$, $p = 0.08$) (see Fig. 3C). No significant correlations were found between EC and STAI scores ($\rho(28) = 0.15$, $p = 0.44$) or between EC and heart rate ($\rho(26) = 0.21$, $p = 0.31$).

3.4. Time courses of subcortical eigenvector centrality

EC time courses of subcortical clusters in the stress and the control group are shown in Fig. 4. The full model that included the *RS-scan* by group interaction and the null model (without the interaction term) differed significantly (likelihood ratio test: $\chi^2(5) = 18.46$, $p < 0.01$). Post-hoc tests showed significantly higher EC values in the stress than in the control group at *rest3* (+35 min; t-ratio (312.18) = -3.40 ; $p < 0.001$) and *rest4* (+55 min; t-ratio (312.18) = -2.49 ; $p < 0.05$). Qualitatively, EC values decreased at 50 min after stressor onset (*rest4*) but then increased again at 85 min (*rest5*) to stay elevated (at least) until 105 min after stress onset (*rest6*). At *rest5* and *rest6*, subcortical EC values in the control group showed a similar increase.

4. Discussion

In this study, we investigated functional brain network topology in response to an acute psychosocial stressor and during the recovery from it. Eigenvector centrality (EC) mapping was used to identify brain hubs involved in stress processing, which were subsequently related to subjective, autonomic, and endocrine stress markers. First, our results show that the TSST elicits strong subjective, autonomic, and endocrine stress responses, as previously described (for a review see Allen et al., 2014). Second, we found an immediate, stress-driven change in whole-brain network topology: EC increased in a cluster peaking in the thalamus, which was connected to regions across the whole brain. This EC increase was more pronounced in participants who also showed stronger stress-related changes in subjective (VAS stressed) as well as – to a lesser extent – autonomic (HRV), and endocrine (saliva cortisol) measures. Third, and different from our expectations based on Hermans et al. (2014), the stress-driven elevation of EC did not recover within 105 min after stress onset. EC values did decrease at 50 min after stressor onset (*rest4*) but then increased again (at least) until the 105 min after stressor onset (*rest6*).

Stress-related changes in brain network topology indicate that thalamic connectivity may be important to information processing immediately after stress exposure. Especially in the immediate aftermath of stress exposure, when the organism is in a hypervigilant state (van

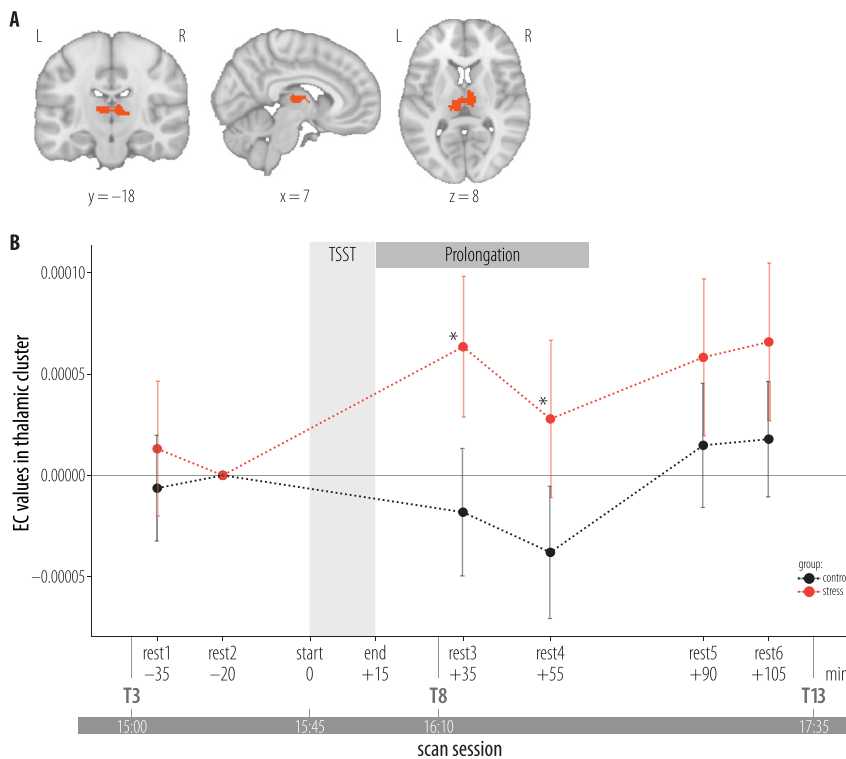


Fig. 4. Thalamic Eigenvector centrality (EC) plotted over the six resting-state (RS) scans. **(A)** Overlap of the RS-scan by group interaction and the simple effect in the stress group (incl. *rest2* and *rest3*), from which EC values were extracted. **(B)** Baseline-corrected (with the value at *rest2*) mean EC values in the cluster shown in A for the six RS scans. Timing relative to TSST onset (start, end, darker grey area). The lighter grey area indicates the time when participants in the stress group were still expecting another task (see section 2.3). After *rest4* (+60 min after TSST onset), they were told that no additional task would follow and that they could relax. The hours indicate the time at which important sampling points were scheduled. There was a significant RS-scan by group interaction ($\chi^2(5) = 18.46$, $p < 0.01$) with significant group differences (stress > control group) at *rest3* (+35 min, t -ratio (312.18) = -3.4; $P_{\text{corr}} < 0.001$) and *rest4* (+55 min, t -ratio (312.18) = -2.49; $P_{\text{corr}} < 0.05$).

Marle et al., 2010), adequate behaviour requires focused resource allocation (e.g., energy supply to brain regions that process relevant information; Hermans et al., 2014). Increased centrality in the thalamus supports its essential role for the control of functional network balance and resource allocation (Garrett et al., 2018; Hwang, Bertolero, Liu, & D'Esposito, 2017). With its extensive structural and functional connectivity, the thalamus is a central relay for sensory signals ascending to the cortex and for trans-thalamic cortico-cortical communication (Sherman and Guillery, 2002). Thalamic nuclei thereby modulate the transfer of information in accord with current attentional and motor or behavioral demands (Sherman and Guillery, 2002; Wolff and Vann, 2019). Beyond being a relay, the thalamus actively and dynamically gates salient inputs by minimizing the importance of currently irrelevant ones (Wolff and Vann, 2019, for review). Activation in the – particularly paraventricular – thalamus has recently been shown to represent salient stimulus features like aversiveness, novelty, and surprise (Zhu et al., 2018). With its inputs from the hypothalamus and brainstem, it also receives information about the homeostatic or arousal state of the organism; and its activation but also its connectivity with cortical regions have been linked to learning processes that underlie behavioral flexibility (Wolff and Vann, 2019; Zhu et al., 2018).

Increased centrality in the thalamus might therefore reflect an increased arousal or alertness (Lohmann et al., 2010; Schiff, 2008) to support the anticipation and processing of salient stimuli (Greenberg et al., 2015; Zhu et al., 2018). The extent of stress effects on brain connectivity is also visible in the results of our exploratory seed-based analysis, showing stress-driven connectivity increases between the thalamic cluster and widespread parietal and temporal regions. Previous studies have shown stress-driven changes in thalamic activation (Dedovic et al., 2014; Fan et al., 2015; Gianaros et al., 2008; Koric et al., 2012; Pruessner et al., 2008; Sinha et al., 2016; Sinha et al., 2004) as well as an increased thalamo-cortical integration with widespread consequences for cortical activity (Maron-Katz et al., 2016) after stressor exposure. While previous stress studies have often also found activation or connectivity changes in the thalamus (but less often discuss them), we did not find significant centrality changes in regions prominent in the stress

literature, like the PFC, the amygdala, the hippocampus, or the hypothalamus. To all these regions, the thalamus is strongly connected (Wolff and Vann, 2019; Zhu et al., 2018) and thalamic EC changes in our study may represent connectivity with these regions (cf. the results of the exploratory seed-based functional connectivity analysis; Fig. S3).

Our results also relate these regions to stress markers beyond the brain: stress-related brain changes in the thalamus were more pronounced in participants with stronger stress responses in subjective stress and – to a lesser extent – peripheral measures (saliva cortisol and heart rate variability). These findings align with evidence that relates thalamic function not only to emotional processing (Barrett, 2016; Kober et al., 2008; Lee et al., 2012; Lee and Shin, 2016; Penzo et al., 2015; Timbie and Barbas, 2015; Wang et al., 2005) but also to homeostatic regulation (Åhs et al., 2009; Cechetto and Shoemaker, 2009; Jaferi and Bhatnagar, 2006; M. M. Suárez and Perassi, 1997; M. Suárez, Maglianesi and Perassi, 1998; Wager et al., 2009; Zhu et al., 2018), showing thalamic involvement for example in the endocrine adaptation to repetitive stressors (Jaferi and Bhatnagar, 2006), respiratory control (Cechetto and Shoemaker, 2009), and parasympathetic cardioregulation (Åhs et al., 2009; Wager et al., 2009). That EC changes were not significantly correlated with changes in STAI scores or HR may suggest that EC alterations are relevant for more stress-specific (VAS, cortisol) and parasympathetic (HRV) than for general anxiety (STAI) or sympathetic (HR) aspects of the stress response.

Besides emotions and homeostasis, our findings can be related to uncertainty. While uncertainty is a crucial component of the TSST and other stressors (de Berker et al., 2016; Koolhaas et al., 2011), according to the free energy principle, the brain constantly tries to match predictions and the environment with the goal of minimizing uncertainty (Friston, 2010; Peters et al., 2017). Thalamic regions – as part of a basal ganglia-thalamo-cortical loop – have been involved in the cognitive processing of uncertainty (Grinband et al., 2006) and in the coordination of “higher” cortical regions (e.g., in prefrontal, insular, and parietal cortices) with the goal to adapt to uncertain environments through probabilistic inferential learning (Mestres-Missé et al., 2017). In general, learning from (stressful) experiences is crucial to reduce uncertainty – and stress – in future situations (de Berker et al., 2016; Peters et al.,

2017). An adaptive stress response thus enables and involves neural plasticity to support these learning processes (Regev and Baram, 2014).

Hallmark of an adaptive stress response is an adequate cortisol response, which, in synergy with other neuroendocrine transmitters, supports rapid behavioural choices but also promotes longer-term neural recovery and higher cognitive functions (Joëls et al., 2013). We thus speculate that our findings can be interpreted as indirect evidence that thalamic are involved in stress-based learning processes (Wolff and Vann, 2019; Zhu et al., 2018). However, as we did not measure such processes, we cannot directly test their relation to the observed EC changes in the thalamus.

Based on the model by Hermans et al. (2014), we anticipated the functional connectivity changes to resemble the time course of the endocrine stress response, increasing immediately after stress exposure and then decaying over time. In the stress group, EC values increased immediately after stress exposure (*rest3*) and decayed during *rest4* (+50 min). However, in both groups, they then increased (again) until the end of the experiment. This pattern may reflect a more general (i.e., group-independent) state (e.g., exhaustion, boredom, annoyance) towards the end of the 6-h experimental procedure. The psychometric measures of stressfulness and exhaustion, which show a similar time course as the EC values in both groups (Fig. 2), support this interpretation. It has been reported that an MRI scan itself can be perceived as stressful (Muehlhan et al., 2011) and the procedure during a RS fMRI acquisition may share some characteristics with the TSST: for example, the participant's "performance" is monitored and recorded by a team of specialists trying to remain and interact in a neutral fashion. Thus, it is conceivable that the observed effects on the neural level are a superposition of two different effects: stress induced by the TSST and the expectation of another task, specific to the stress group and with a clear cortisol response, and exhaustion/boredom/annoyance in both groups, caused by the overall length of the experiment. For the last scan (*rest6*), the control group reported significantly higher state anxiety and subjective stress than the stress group (while the autonomic and endocrine stress markers did not "flip"). This illustrates that physiological and subjective stress measures can – and often do – dissociate (D. Hellhammer, Stone, Hellhammer and Broderick, 2010; J. Hellhammer and Schubert, 2012).

There are several limitations that should be considered when interpreting the findings of our study: we only included young, healthy, male participants. While this allowed us to investigate stress-induced changes using a multimodal approach without confounds like the impact of the ovarian cycle, the generalisability of our results has to be tested in studies with more heterogeneous samples. To sample female participants at the same phase of the ovarian cycle would have been beyond the resources of our study as self-reports or (single) assessments of physiological parameters (e.g., body temperature, hormone concentrations) are unreliable and, for example, highly influenced by day-to-day fluctuations (cf. Barth et al., 2016). Our study design cannot disentangle the aspects of increased thalamic centrality that are due to more general changes in alertness or arousal from those that are stress-specific. That there is a stress-specific component is suggested by the association of EC increases with dedicated stress markers like subjective stress or - to a lesser extent - saliva cortisol and by the absence of a group difference in self-reported alertness (non-significant *RS-scan* by *group* interaction in a linear mixed model of the mood scale's sleepiness component; Dalbert, 1992; Fig. S2). Although the TSST's strong and long lasting effect was crucial for our research question, it does not include a parametric modulation of the stressor (e.g., by varying levels of uncertainty; de Berker et al., 2016), which would provide a more fine-grained analysis of the association between stress-inducing uncertainty and, for example, thalamic network centrality. In addition, the functional significance of centrality changes could be confirmed by including a task after the stressor, which allows, for example, the measurement of attentional performance. Please note that our results show the network hubs based on EC across voxels - but not regions - in the brain. Treating each voxel as an independent unit

might bias the results because of the different size of different brain regions. However, atlas-based network analyses depend on prior assumptions about functional brain topology, which can also bias the results (de Reus & van den Heuvel, 2013).

In this study, we show stress-driven changes in whole-brain functional network topology without a priori definition of seed regions or network masks. By acquiring data from different stress systems over an extended time after stressor onset, it was possible to not just modally investigate immediate stress effects but also their time courses during recovery. We identified thalamic regions to be centrally involved in the neural response to acute stress, underlying stress-related connectivity changes across the whole brain. Changes in thalamic centrality were also related to subjective as well as – to a lesser extent – to autonomic and endocrine stress measures. The importance of the thalamus supports the hypothesis that acute stress shifts resources towards a state of heightened saliency processing. The thalamus may thus be a target for future research – also investigating stress-related psychopathology, such as post-traumatic stress disorder (Yin et al., 2011), depression (Greicius et al., 2007), addiction (Everitt and Robbins, 2013), or schizophrenia (Giraldo-Chica and Woodward, 2017; Howes et al., 2017). Of particular importance is also the role of stress resilience (Brown et al., 2014), which requires studying the time course of the brain's response to stress and its association with peripheral stress markers. In conclusion, our findings suggest thalamic connectivity to play a central role for the processing of stress and to constitute a nexus for stress responses in the rest of the body and in the mind.

Funding

This research did not receive any specific grant from funding agencies in the public, commercial, or not-for-profit sectors.

Acknowledgments

The authors would like to thank Dr. Ilya Veer and Dr. Robert Nadon for helpful methodological discussions. MG was funded by the German Federal Ministry of Education and Research (grant no. 13GW0206B).

Appendix A. Supplementary data

Supplementary data to this article can be found online at <https://doi.org/10.1016/j.neuroimage.2019.06.005>.

References

- Åhs, F., Sollers, J.J., Furmark, T., Fredrikson, M., Thayer, J.F., 2009. High-frequency heart rate variability and cortico-striatal activity in men and women with social phobia. *Neuroimage* 47 (3), 815–820. <https://doi.org/10.1016/j.neuroimage.2009.05.091>.
- al'Absi, M., Lovallo, W.R., McKey, B., Sung, B.H., Whitsett, T.L., Wilson, M.F., 1998. Hypothalamic-pituitary-adrenocortical responses to psychological stress and caffeine in men at high and low risk for hypertension. *Psychosom. Med.* 60 (4), 521–527.
- Allen, A.P., Kennedy, P.J., Cryan, J.F., Dinan, T.G., Clarke, G., 2014. Biological and psychological markers of stress in humans: focus on the trier social stress test. *Neurosci. Biobehav. Rev.* 38, 94–124. <https://doi.org/10.1016/j.neubiorev.2013.11.005>.
- Allen, A.P., Kennedy, P.J., Dockray, S., Cryan, J.F., Dinan, T.G., Clarke, G., 2017. The trier social stress test: principles and practice. *Neurobiol. Stress* 6, 113–126. <https://doi.org/10.1016/j.ynstr.2016.11.001>.
- Avants, B.B., Tustison, N.J., Song, G., Cook, P.A., Klein, A., Gee, J.C., 2011. A reproducible evaluation of ANTs similarity metric performance in brain image registration. *Neuroimage* 54 (3), 2033–2044. <https://doi.org/10.1016/j.neuroimage.2010.09.025>.
- Baayen, R. Harald, 2008. *Analyzing Linguistic Data: A Practical Introduction to Statistics Using R*. Cambridge University Press.
- Babayan, A., Erbey, M., Kumral, D., Reinelt, J.D., Reiter, A.M.F., Röbbig, J., et al., 2019. A mind-brain-body dataset of MRI, EEG, cognition, emotion, and peripheral physiology in young and old adults. *Sci. Data* 6, 180308. <https://doi.org/10.1038/sdata.2018.308>.
- Bae, Y.J., Reinelt, J., Netto, J., Uhlig, M., Willenberg, A., Ceglarek, U., et al., 2019. Salivary cortisone, as a biomarker for psychosocial stress, is associated with state anxiety and heart rate. *Psychoneuroendocrinology* 101, 35–41. <https://doi.org/10.1016/j.psyneuen.2018.10.015>.

- Bansal, R., Peterson, B.S., 2018. Cluster-level statistical inference in fMRI datasets: the unexpected behavior of random fields in high dimensions. *Magn. Reson. Imag.* 49, 101–115. <https://doi.org/10.1016/j.mri.2018.01.004>.
- Barrett, L.F., 2016. The theory of constructed emotion: an active inference account of interoception and categorization. *Soc. Cognit. Affect Neurosci.* nsw154 <https://doi.org/10.1093/scan/nsw154>.
- Barth, C., Steele, C.J., Mueller, K., Rekkas, V.P., Arélin, K., Pampel, A., et al., 2016. In-vivo dynamics of the human Hippocampus across the menstrual cycle. *Sci. Rep.* 6, 32833. <https://doi.org/10.1038/srep32833>.
- Bates, D., Mächler, M., Bolker, B., Walker, S., 2015. Fitting linear mixed-effects models using lme4. *J. Stat. Softw.* 67 (1), 1–48. <https://doi.org/10.18637/jss.v067.i01>.
- Berntson, G.G., Bigger, J.T., Eckberg, D.L., Grossman, P., Kaufmann, P.G., Malik, M., et al., 1997. Heart rate variability: origins, methods, and interpretive caveats. *Psychophysiology* 34 (6), 623–648.
- Brown, V.M., LaBar, K.S., Haswell, C.C., Gold, A.L., Mid-Atlantic MIRECC Workgroup, McCarthy, G., Morey, R.A., 2014. Altered resting-state functional connectivity of basolateral and centromedial amygdala complexes in posttraumatic stress disorder. *Neuropsychopharmacology: Official Publication of the American College of Neuropsychopharmacology* 39 (2), 351–359. <https://doi.org/10.1038/npp.2013.197>.
- Cechetto, D.F., Shoemaker, J.K., 2009. Functional neuroanatomy of autonomic regulation. *Neuroimage* 47 (3), 795–803. <https://doi.org/10.1016/j.neuroimage.2009.05.024>.
- Childs, E., Dlugos, A., De Wit, H., 2010. Cardiovascular, hormonal, and emotional responses to the TSSST in relation to sex and menstrual cycle phase. *Psychophysiology* 47 (3), 550–559. <https://doi.org/10.1111/j.1469-8986.2009.00961.x>.
- Dalbert, C., 1992. Subjektives Wohlbefinden junger Erwachsener: theoretische und empirische Analysen der Struktur und Stabilität. [Young adults' subjective well-being: theoretical and empirical analyses of its structure and stability.]. *Z. Differ. Diagn. Psychol.* 13 (4), 207–220.
- de Berker, A.O., Rutledge, R.B., Mathys, C., Marshall, L., Cross, G.F., Dolan, R.J., Bestmann, S., 2016. Computations of uncertainty mediate acute stress responses in humans. *Nat. Commun.* 7 (1). <https://doi.org/10.1038/ncomms10996>.
- de Reus, M.A., van den Heuvel, M.P., 2013. The parcellation-based connectome: limitations and extensions. *Neuroimage* 80, 397–404. <https://doi.org/10.1016/j.neuroimage.2013.03.053>.
- Dedovic, K., Duchesne, A., Engert, V., Lue, S.D., Andrews, J., Efanov, S.I., et al., 2014. Psychological, endocrine and neural responses to social evaluation in subclinical depression. *Soc. Cognit. Affect Neurosci.* 9 (10), 1632–1644. <https://doi.org/10.1093/scan/nst151>.
- Dobson, Annette J., Barnett, Adrian G., 2018. *An Introduction to Generalized Linear Models*.
- Everitt, B.J., Robbins, T.W., 2013. From the ventral to the dorsal striatum: devolving views of their roles in drug addiction. *Neurosci. Biobehav. Rev.* 37 (9 Pt A), 1946–1954. <https://doi.org/10.1016/j.neubiorev.2013.02.010>.
- Fan, Y., Pestke, K., Feeser, M., Aust, S., Pruessner, J.C., Böker, H., et al., 2015. Amygdala–Hippocampal connectivity changes during acute psychosocial stress: joint effect of early life stress and oxytocin. *Neuropsychopharmacology* 40 (12), 2736–2744. <https://doi.org/10.1038/npp.2015.123>.
- Faravelli, C., Lo Sauro, C., Godini, L., Lelli, L., Benni, L., Pietrini, F., et al., 2012. Childhood stressful events, HPA axis and anxiety disorders. *World J. Psychiatr.* 2 (1), 13–25. <https://doi.org/10.5498/wjp.v2.i1.13>.
- Fehm, L., Hoyer, J., Schneider, G., Lindemann, C., Klusmann, U., 2008. Assessing post-event processing after social situations: a measure based on the cognitive model for social phobia. *Anxiety Stress Coping* 21 (2), 129–142. <https://doi.org/10.1080/10615800701424672>.
- Forstmeier, W., Schielzeth, H., 2011. Cryptic multiple hypotheses testing in linear models: overestimated effect sizes and the winner's curse. *Behav. Ecol. Sociobiol.* 65 (1), 47–55. <https://doi.org/10.1007/s00265-010-1038-5>.
- Friston, K., 2010. The free-energy principle: a unified brain theory? *Nat. Rev. Neurosci.* 11 (2), 127–138. <https://doi.org/10.1038/nrn2787>.
- Garrett, D., Epp, S., Perry, A., Lindenberger, U., 2018. Local temporal variability reflects functional network integration in the human brain: on the crucial role of the thalamus. *BioRxiv*. <https://doi.org/10.1101/184739>.
- Gaudl, A., Kratzsch, J., Bae, Y.-J., Kiess, W., Thiery, J., Ceglarek, U., 2016. Liquid chromatography quadrupole linear ion trap mass spectrometry for quantitative steroid hormone analysis in plasma, urine, saliva and hair. *J. Chromatogr. A* 1464, 64–71. <https://doi.org/10.1016/j.chroma.2016.07.087>.
- Gianaros, P.J., Sheu, L.K., Matthews, K.A., Jennings, J.R., Manuck, S.B., Hariri, A.R., 2008. Individual differences in stressor-evoked blood pressure reactivity vary with activation, volume, and functional connectivity of the amygdala. *J. Neurosci.* 28 (4), 990–999. <https://doi.org/10.1523/JNEUROSCI.3606-07.2008>.
- Giraldo-Chica, M., Woodward, N.D., 2017. Review of thalamocortical resting-state fMRI studies in schizophrenia. *Schizophr. Res.* 180, 58–63. <https://doi.org/10.1016/j.schres.2016.08.005>.
- Gorgolewski, K., Burns, C.D., Madison, C., Clark, D., Halchenko, Y.O., Waskom, M.L., Ghosh, S.S., 2011. Nipype: a flexible, lightweight and extensible neuroimaging data processing framework in python. *Front. Neuroinf.* 5, 13. <https://doi.org/10.3389/fninf.2011.00013>.
- Greenberg, T., Carlson, J.M., Rubin, D., Cha, J., Mujica-Parodi, L., 2015. Anticipation of high arousal aversive and positive movie clips engages common and distinct neural substrates. *Soc. Cognit. Affect Neurosci.* 10 (4), 605–611. <https://doi.org/10.1093/scan/nsu091>.
- Greicius, M.D., Flores, B.H., Menon, V., Glover, G.H., Solvason, H.B., Kenna, H., et al., 2007. Resting-state functional connectivity in major depression: abnormally increased contributions from subgenual cingulate cortex and thalamus. *Biol. Psychiatry* 62 (5), 429–437. <https://doi.org/10.1016/j.biopsych.2006.09.020>.
- Grimm, S., Ernst, J., Boesiger, P., Schuepbach, D., Hell, D., Boeker, H., Northoff, G., 2009. Increased self-focus in major depressive disorder is related to neural abnormalities in subcortical-cortical midline structures. *Hum. Brain Mapp.* 30 (8), 2617–2627. <http://doi.org/10.1002/hbm.20693>.
- Grinband, J., Hirsch, J., Ferrera, V.P., 2006. A neural representation of categorization uncertainty in the human brain. *Neuron* 49 (5), 757–763. <https://doi.org/10.1016/j.neuron.2006.01.032>.
- Hellhammer, D., Stone, A., Hellhammer, J., Broderick, J., 2010. Measuring stress. *Encycl. Behav. Neurosci.* 2, 186–191.
- Hellhammer, J., Schubert, M., 2012. The physiological response to Trier Social Stress Test relates to subjective measures of stress during but not before or after the test. *Psychoneuroendocrinology* 37 (1), 119–124. <https://doi.org/10.1016/j.psychoneu.2011.05.012>.
- Hermans, E.J., Henckens, M.J.A.G., Joëls, M., Fernández, G., 2014. Dynamic adaptation of large-scale brain networks in response to acute stressors. *Trends Neurosci.* 37 (6), 304–314. <https://doi.org/10.1016/j.tins.2014.03.006>.
- Het, S., Rohleder, N., Schoofs, D., Kirschbaum, C., Wolf, O.T., 2009. Neuroendocrine and psychometric evaluation of a placebo version of the 'trier social stress test'. *Psychoneuroendocrinology* 34 (7), 1075–1086. <https://doi.org/10.1016/j.psychoneu.2009.02.008>.
- Howes, O.D., McCutcheon, R., Owen, M.J., Murray, R.M., 2017. The role of genes, stress, and dopamine in the development of schizophrenia. *Biol. Psychiatry* 81 (1), 9–20. <https://doi.org/10.1016/j.biopsych.2016.07.014>.
- Hwang, K., Bertolero, M.A., Liu, W.B., D'Esposito, M., 2017. The human thalamus is an integrative hub for functional brain networks. *J. Neurosci.* 37 (23), 5594–5607. <https://doi.org/10.1523/JNEUROSCI.0067-17.2017>.
- Jaferi, A., Bhatnagar, S., 2006. Corticosterone can act at the posterior paraventricular thalamus to inhibit hypothalamic-pituitary-adrenal activity in animals that habituate to repeated stress. *Endocrinology* 147 (10), 4917–4930. <https://doi.org/10.1210/en.2005-1393>.
- Joëls, M., Pasricha, N., Karst, H., 2013. The interplay between rapid and slow corticosteroid actions in brain. *Eur. J. Pharmacol.* 719 (1–3), 44–52. <https://doi.org/10.1016/j.ejphar.2013.07.015>.
- Joyce, K.E., Laurienti, P.J., Burdette, J.H., Hayasaka, S., 2010. A new measure of centrality for brain networks. *PLoS One* 5 (8), e12200. <https://doi.org/10.1371/journal.pone.0012200>.
- Killgore, W.D., 1998. The Affect Grid: a moderately valid, nonspecific measure of pleasure and arousal. *Psychol. Rep.* 83 (2), 639–642. <https://doi.org/10.2466/pr0.1998.83.2.639>.
- Kirschbaum, C., Pirke, K.-M., Hellhammer, D.H., 1993. The 'trier social stress test' – a tool for investigating psychobiological stress responses in a laboratory setting. *Neuroendocrinology* 28 (1–2), 76–81.
- Klein, E.M., Brähler, E., Dreier, M., Reinecke, L., Müller, K.W., Schmutz, G., et al., 2016. The German version of the Perceived Stress Scale - psychometric characteristics in a representative German community sample. *BMC Psychiatry* 16, 159. <https://doi.org/10.1186/s12888-016-0875-9>.
- Kober, H., Barrett, L.F., Joseph, J., Bliss-Moreau, E., Lindquist, K., Wager, T.D., 2008. Functional grouping and cortical-subcortical interactions in emotion: a meta-analysis of neuroimaging studies. *Neuroimage* 42 (2), 998–1031. <https://doi.org/10.1016/j.neuroimage.2008.03.059>.
- Koolhaas, J.M., Bartolomucci, A., Buwalda, B., de Boer, S.F., Flügge, G., Korte, S.M., et al., 2011. Stress revisited: a critical evaluation of the stress concept. *Neurosci. Biobehav. Rev.* 35 (5), 1291–1301. <https://doi.org/10.1016/j.neubiorev.2011.02.003>.
- Koric, L., Volle, E., Seassau, M., Bernard, F.A., Mancini, J., Dubois, B., et al., 2012. How cognitive performance-induced stress can influence right VLPFC activation: an fMRI study in healthy subjects and in patients with social phobia. *Hum. Brain Mapp.* 33 (8), 1973–1986. <https://doi.org/10.1002/hbm.21340>.
- Lee, S., Ahmed, T., Lee, S., Kim, H., Choi, S., Kim, D.-S., et al., 2012. Bidirectional modulation of fear extinction by mediadorsal thalamic firing in mice. *Nat. Neurosci.* 15 (2), 308–314. <https://doi.org/10.1038/nn.2999>.
- Lee, S., Shin, H.-S., 2016. The role of mediadorsal thalamic nucleus in fear extinction. *J. Anal. Sci. Technol.* 7 (1). <https://doi.org/10.1186/s40543-016-0093-6>.
- Lenth, R., Singmann, H., Love, J., Buerkner, P., Herve, M., 2018. *Emmeans: Estimated Marginal Means, Aka Least-Squares Means (Version 1.1.3)*. Retrieved from. <https://CRAN.R-project.org/package=emmeans>.
- Linden, W., Earle, T.L., Gerin, W., Christenfeld, N., 1997. Physiological stress reactivity and recovery: conceptual siblings separated at birth? *J. Psychosom. Res.* 42 (2), 117–135. [https://doi.org/10.1016/S0022-3999\(96\)00240-1](https://doi.org/10.1016/S0022-3999(96)00240-1).
- Lohmann, G., Margulies, D.S., Horstmann, A., Pleger, B., Lepsien, J., Goldhahn, D., et al., 2010. Eigenvector centrality mapping for analyzing connectivity patterns in fMRI data of the human brain. *PLoS One* 5 (4), e10232. <https://doi.org/10.1371/journal.pone.0010232>.
- Maron-Katz, A., Vaisvaser, S., Lin, T., Hendler, T., Shamir, R., 2016. A large-scale perspective on stress-induced alterations in resting-state networks. *Sci. Rep.* 6 (1). <https://doi.org/10.1038/srep21503>.
- Marques, J.P., Kober, T., Krueger, G., van der Zwaag, W., Van de Moortele, P.-F., Gruetter, R., 2010. MP2RAGE, a self bias-field corrected sequence for improved segmentation and T1-mapping at high field. *Neuroimage* 49 (2), 1271–1281. <https://doi.org/10.1016/j.neuroimage.2009.10.002>.
- Mathôt, S., Schrei, D., Theeuwes, J., 2011. OpenSesame: an open-source, graphical experiment builder for the social sciences. *Behav. Res. Methods* 44 (2), 314–324. <https://doi.org/10.3758/s13428-011-0168-7>.
- McEwen, B.S., Gianaros, P.J., 2011. Stress- and allostasis-induced brain plasticity. *Annu. Rev. Med.* 62 (1), 431–445. <https://doi.org/10.1146/annurev-med-052209-100430>.

- Mendes, N., Oligschläger, S., Lauckner, M.E., Golchert, J., Huntenburg, J.M., Falkiewicz, M., et al., 2019. A functional connectome phenotyping dataset including cognitive state and personality measures. *Sci. Data* 6, 180307. <https://doi.org/10.1038/sdata.2018.307>.
- Mestres-Missé, A., Trampel, R., Turner, R., Kotz, S.A., 2017. Uncertainty and expectancy deviations require cortico-subcortical cooperation. *Neuroimage* 144 (Pt A), 23–34. <https://doi.org/10.1016/j.neuroimage.2016.05.069>.
- Miller, R., Plessow, F., Kirschbaum, C., Stalder, T., 2013. Classification criteria for distinguishing cortisol responders from nonresponders to psychosocial stress: evaluation of salivary cortisol pulse detection in panel designs. *Psychosom. Med.* 75 (9), 832–840. <https://doi.org/10.1097/PSY.000000000000002>.
- Muehlhan, M., Lueken, U., Wittchen, H.-U., Kirschbaum, C., 2011. The scanner as a stressor: evidence from subjective and neuroendocrine stress parameters in the time course of a functional magnetic resonance imaging session. *Int. J. Psychophysiol.* 79 (2), 118–126. <https://doi.org/10.1016/j.ijpsycho.2010.09.009>.
- Mueller, K., Jech, R., Hoskocová, M., Ulmanová, O., Uργοšik, D., Vymazal, J., Růžicka, E., 2017. General and selective brain connectivity alterations in essential tremor: a resting state fMRI study. *NeuroImage. Clinical* 16, 468–476. <https://doi.org/10.1016/j.nicl.2017.06.004>.
- Nichols, T., Hayasaka, S., 2003. Controlling the familywise error rate in functional neuroimaging: a comparative review. *Stat. Methods Med. Res.* 12 (5), 419–446. <https://doi.org/10.1191/0962280203sm341ra>.
- Nierhaus, T., Gundlach, C., Goltz, D., Thiel, S.D., Pleger, B., Villringer, A., 2013. Internal ventilation system of MR scanners induces specific EEG artifact during simultaneous EEG-fMRI. *Neuroimage* 74, 70–76. <https://doi.org/10.1016/j.neuroimage.2013.02.016>.
- Penzo, M.A., Robert, V., Tucciarone, J., De Bundel, D., Wang, M., Van Aelst, L., et al., 2015. The paraventricular thalamus controls a central amygdala fear circuit. *Nature* 519 (7544), 455–459. <https://doi.org/10.1038/nature13978>.
- Peters, A., McEwen, B.S., Friston, K., 2017. Uncertainty and stress: why it causes diseases and how it is mastered by the brain. *Prog. Neurobiol.* 156, 164–188. <https://doi.org/10.1016/j.pneurobio.2017.05.004>.
- Phillips, C., 2016. *SPM Cluster Size Threshold Estimation* [Matlab]. Retrieved from: https://github.com/CyclotronResearchCentre/SPM_ClusterSizeThreshold (Original work published 2016).
- Pittenger, C., Duman, R.S., 2008. Stress, depression, and neuroplasticity: a convergence of mechanisms. *Neuropsychopharmacology: Off. Publ. Am. Coll. Neuropsychopharmacol.* 33 (1), 88–109. <https://doi.org/10.1038/sj.npp.1301574>.
- Power, J.D., Barnes, K.A., Snyder, A.Z., Schlaggar, B.L., Petersen, S.E., 2012. Spurious but systematic correlations in functional connectivity MRI networks arise from subject motion. *Neuroimage* 59 (3), 2142–2154. <https://doi.org/10.1016/j.neuroimage.2011.10.018>.
- Pruessner, J.C., Dedovic, K., Khalili-Mahani, N., Engert, V., Pruessner, M., Buss, C., et al., 2008. Deactivation of the limbic system during acute psychosocial stress: evidence from positron emission tomography and functional magnetic resonance imaging studies. *Biol. Psychiatry* 63 (2), 234–240. <https://doi.org/10.1016/j.biopsych.2007.04.041>.
- Quaedflieg, C.W.E.M., van de Ven, V., Meyer, T., Siep, N., Merckelbach, H., Smeets, T., 2015. Temporal dynamics of stress-induced alterations of intrinsic amygdala connectivity and neuroendocrine levels. *PLoS One* 10 (5), e0124141. <https://doi.org/10.1371/journal.pone.0124141>.
- Rack-Gomer, A.L., Liau, J., Liu, T.T., 2009. Caffeine reduces resting-state BOLD functional connectivity in the motor cortex. *Neuroimage* 46 (1), 56–63. <https://doi.org/10.1016/j.neuroimage.2009.02.001>.
- R Development Core Team, 2008. *R: A language and environment for statistical computing*.
- Regev, L., Baram, T.Z., 2014. Corticotropin releasing factor in neuroplasticity. *Front. Neuroendocrinol.* 35 (2), 171–179. <https://doi.org/10.1016/j.yfne.2013.10.001>.
- Rubinov, M., Sporns, O., 2010. Complex network measures of brain connectivity: uses and interpretations. *Neuroimage* 52 (3), 1059–1069. <https://doi.org/10.1016/j.neuroimage.2009.10.003>.
- Schiff, N.D., 2008. Central thalamic contributions to arousal regulation and neurological disorders of consciousness. *Ann. N. Y. Acad. Sci.* 1129 (1), 105–118. <https://doi.org/10.1196/annals.1417.029>.
- Schulz, P., Schlotz, W., 1999. Trierer Inventar zur Erfassung von chronischem Sre (TICS): skalenkonstruktion, teststatistische Überprüfung und Validierung der Skala Arbeitsüberlastung. [The Trier Inventory for the Assessment of Chronic Stress (TICS). Scale construction, statistical testing, and validation of the scale work overload.]. *Diagnostica* 45 (1), 8–19. <https://doi.org/10.1026//0012-1924.45.1.8>.
- Sherman, S.M., Guillery, R.W., 2002. The role of the thalamus in the flow of information to the cortex. *Phil. Trans. Biol. Sci.* 357 (1428), 1695–1708. <https://doi.org/10.1098/rstb.2002.1161>.
- Sinha, R., Lacadie, C.M., Constable, R.T., Seo, D., 2016. Dynamic neural activity during stress signals resilient coping. *Proc. Natl. Acad. Sci. Unit. States Am.* 113 (31), 8837–8842. <https://doi.org/10.1073/pnas.1600965113>.
- Sinha, R., Lacadie, C., Skudlarski, P., Wexler, B.E., 2004. Neural circuits underlying emotional distress in humans. *Ann. N. Y. Acad. Sci.* 1032 (1), 254–257. <https://doi.org/10.1196/annals.1314.032>.
- Smith, S.M., Jenkinson, M., Woolrich, M.W., Beckmann, C.F., Behrens, T.E.J., Johansen-Berg, H., et al., 2004. Advances in functional and structural MR image analysis and implementation as FSL. *Neuroimage* 23 (Suppl. 1), S208–S219. <https://doi.org/10.1016/j.neuroimage.2004.07.051>.
- Spielberger, C.D., 1983. Manual for the State-Trait Anxiety Inventory STAI (Form Y) (“Self-Evaluation Questionnaire”). Retrieved from: <http://ubir.buffalo.edu/xmlui/handle/10477/1873>.
- Steptoe, A., Kivimäki, M., 2013. Stress and cardiovascular disease: an update on current knowledge. *Annu. Rev. Public Health* 34 (1), 337–354. <https://doi.org/10.1146/annurev-publichealth-031912-114452>.
- Suárez, M.M., Perassi, N.I., 1997. Influence of anterodorsal thalamic nuclei on ACTH release under basal and stressful conditions. *Physiol. Behav.* 62 (2), 373–377.
- Suárez, M., Maglianesi, M.A., Perassi, N.I., 1998. Involvement of the anterodorsal thalamic nuclei on the hypophysoadrenal response to chronic stress in rats. *Physiol. Behav.* 64 (1), 111–116.
- Tarvainen, M.P., Niskanen, J.-P., Lipponen, J.A., Ranta-Aho, P.O., Karjalainen, P.A., 2014. Kubios HRV—heart rate variability analysis software. *Comput. Methods Progr. Biomed.* 113 (1), 210–220. <https://doi.org/10.1016/j.cmpb.2013.07.024>.
- Timbie, C., Barbas, H., 2015. Pathways for emotions: specializations in the amygdalar, mediodorsal thalamic, and posterior orbitofrontal network. *J. Neurosci.: Off. J. Soc. Neurosci.* 35 (34), 11976–11987. <https://doi.org/10.1523/JNEUROSCI.2157-15.2015>.
- Vaisvaser, S., Lin, T., Admon, R., Podlipsky, I., Greenman, Y., Stern, N., et al., 2013. Neural traces of stress: cortisol related sustained enhancement of amygdala-hippocampal functional connectivity. *Front. Hum. Neurosci.* 7. <https://doi.org/10.3389/fnhum.2013.00313>.
- van Marle, H.J.F., Hermans, E.J., Qin, S., Fernández, G., 2010. Enhanced resting-state connectivity of amygdala in the immediate aftermath of acute psychological stress. *Neuroimage* 53 (1), 348–354. <https://doi.org/10.1016/j.neuroimage.2010.05.070>.
- van Oort, J., Tendolcar, I., Hermans, E.J., Mulders, P.C., Beckmann, C.F., Schene, A.H., et al., 2017. How the brain connects in response to acute stress: a review at the human brain systems level. *Neurosci. Biobehav. Rev.* 83, 281–297. <https://doi.org/10.1016/j.neubiorev.2017.10.015>.
- Veer, I.M., Oei, N.Y.L., Spinhoven, P., van Buchem, M.A., Elzinga, B.M., Rombouts, S.A.R.B., 2011. Beyond acute social stress: increased functional connectivity between amygdala and cortical midline structures. *Neuroimage* 57 (4), 1534–1541. <https://doi.org/10.1016/j.neuroimage.2011.05.074>.
- Wager, T.D., van Ast, V.A., Hughes, B.L., Davidson, M.L., Lindquist, M.A., Ochsner, K.N., 2009. Brain mediators of cardiovascular responses to social threat, Part II: prefrontal-subcortical pathways and relationship with anxiety. *Neuroimage* 47 (3), 836–851. <https://doi.org/10.1016/j.neuroimage.2009.05.044>.
- Wang, J., Rao, H., Wetmore, G.S., Furlan, P.M., Kerczykowski, M., Dinges, D.F., Detre, J.A., 2005. Perfusion functional MRI reveals cerebral blood flow pattern under psychological stress. *Proc. Natl. Acad. Sci. Unit. States Am.* 102 (49), 17804–17809. <https://doi.org/10.1073/pnas.0503082102>.
- Wellcome Trust Centre. (n.d.). SPM12 - Statistical Parametric Mapping - by Members & Collaborators of the Wellcome Centre for Human Neuroimaging. Retrieved from <https://www.fil.ion.ucl.ac.uk/spm/software/spm12/>
- Wheelock, M.D., Rangaprakash, D., Harnett, N.G., Wood, K.H., Orem, T.R., Mrug, S., et al., 2018. Psychosocial stress reactivity is associated with decreased whole-brain network efficiency and increased amygdala centrality. *Behav. Neurosci.* 132 (6), 561–572. <https://doi.org/10.1037/bne0000276>.
- Wink, A.M., de Munck, J.C., van der Werf, Y.D., van den Heuvel, O.A., Barkhof, F., 2012. Fast eigenvector centrality mapping of voxel-wise connectivity in functional magnetic resonance imaging: implementation, validation, and interpretation. *Brain Connect.* 2 (5), 265–274. <https://doi.org/10.1089/brain.2012.0087>.
- Wolff, M., Vann, S.D., 2019. The cognitive thalamus as a gateway to mental representations. *J. Neurosci.: Off. J. Soc. Neurosci.* 39 (1), 3–14. <https://doi.org/10.1523/JNEUROSCI.0479-18.2018>.
- Yin, Y., Jin, C., Hu, X., Duan, L., Li, Z., Song, M., et al., 2011. Altered resting-state functional connectivity of thalamus in earthquake-induced posttraumatic stress disorder: a functional magnetic resonance imaging study. *Brain Res.* 1411, 98–107. <https://doi.org/10.1016/j.brainres.2011.07.016>.
- Zhu, Y., Nachtrab, G., Keyes, P.C., Allen, W.E., Luo, L., Chen, X., 2018. Dynamic salience processing in paraventricular thalamus gates associative learning. *Science* 362 (6413), 423–429. <https://doi.org/10.1126/science.aat0481>.